

SCALE EFFECT AT TRANSONIC FLOW PAST A SWEEP THICK
SUPERCRITICAL HIGH-ASPECT-RATIO WING.

ICAS-94-3.8.4

V.D.Bokser
Central Aerohydrodynamic Institute,
(TsAGI), Zhukovsky, Russia.

Abstract

The aerodynamic features of the thick ($\bar{c} = 15; 13; 11\%$) swept ($\chi_{\bar{M}_\infty} 30^\circ$) high-aspect-ratio ($AR = 10$) wing incorporating supercritical second-generation airfoil sections in transonic flow regimes ($M = 0.6$ to $0.85, \alpha = -1^\circ$ to 12°) Reynolds number up to $Re_{max} = 32 \cdot 10^6$ are studied on a large-scale semi-span wing-body model.

The peculiarities of the pressure distribution, lifting capabilities of wing sections under both subcritical and supercritical flow conditions are examined. Also considered are distinctive features of developing local supersonic region on the supercritical wing incorporating thick supercritical second-generation airfoil sections. Attached and separated flow regimes as well as the effect of Reynolds number on suppressing flow separation in various wing sections are investigated.

Nomenclature.

b - wing section chord;
 \bar{c} - maximum wing section thickness-to-chord ratio;
 C_p - pressure coefficient;
 $C_{p_{cr}}$ - critical value of pressure coefficient;
 $C_{p_{t.e.}}$ - pressure coefficient at wing section trailing edge;
CL - wing lift coefficient;
Cl - section lift coefficient;
CLal. - allowed wing lift coefficient;
Clal. - allowed section lift coefficient;

CLcru. - cruise wing lift coefficient;
CL α - wing lift curve slope;
Cl α - section lift curve slope;
M - freestream Mach number;
Msh - local Mach number in front of the shock wave at the wing surface;
Re - Reynolds number;
 $\alpha_{sep.}$ - angle of attack corresponding to the onset of flow separation;
CLsep. - wing lift coefficient corresponding to the onset of flow separation;
 $\bar{x} = x/b$ - dimensionless chordwise coordinate;
 \bar{x}_{sh} - section chordwise shock position;
 $\bar{z} = 2z/l$ - dimensionless spanwise section location;
 $\bar{z}_{t.e.k}$ - dimensionless coordinate of the trailing edge kink;
 \bar{z}_{sep} - dimensionless coordinate of the wing section where separation originates;
 χ - wing sweep angle.

Introduction

The wings of moderate sweep angles ($\chi_{M_\infty} < 30^\circ$) and high aspect ratios (up to $AR = 10$ and above) incorporating supercritical airfoil sections with various thickness-to-chord ratios find extensive application in designing economically efficient passenger and cargo transport aircraft.

The use of supercritical airfoils particularly the second-generation ones, in

designing swept wings generates an imperative used for flow conditions close to the full-scale one to be duplicated in wind-tunnel experiments. The investigation of the scale effect is of importance regarding both the cruise flight regime ((L/D)_{max} problem) and the regime of the onset and development of boundary-layer separation (problems of CL₁, CL_{max}, pitch-up tendency which exhibit moment versus alpha curves, and so on).

Investigations using sophisticated methods of measurement and visualization formerly carried out at TsAGI on the features of transonic flowfields over classical-type and supercritical (V.D. Bokser, G.A. Pavlovets) airfoils at high Reynolds numbers (up to Re = 25*10⁶) have revealed a scale effect substantially influencing the development of a local supersonic region and the suppression of boundary-layer separation. (1)

The use of supercritical airfoil in designing a swept wing essentially alters the character of the Reynolds number influence on its flowfield. It is advisable to examine this phenomenon in wind-tunnels on large-scale semi-span models (2,3)

Flow-visualization studies performed at TsAGI at transonic speeds on supercritical airfoils with thickness-to-chord ratios of $\bar{c} = 14.5; 10; 9\%$ using the large-scale semi-model with the wing of sufficiently high sweep angle ($\gamma_{1/4} = 35^\circ$) and moderate aspect ratio (AR = 7.5) identified a number of essential aerodynamic features which manifest themselves under high Reynolds number conditions (2).

The purpose of the present work is to investigate the aerodynamic peculiarities of thick ($\bar{c} = 15; 13; 11\%$) second-generation supercritical airfoils incorporated in the

wing of moderate sweep angle ($\gamma_{1/4} = 30^\circ$) high aspect ratio (AR = 10) with built-in twists of $\epsilon = 0, -3^\circ$ and -4° at transonic flow conditions with Reynolds numbers of up to Re = 32*10⁶.

Testing technique.

Experimental study on the influence of Reynolds number on aerodynamics of a supercritical wing was carried out in the transonic wind-tunnel on the semi-span wing-fuselage model with high-density pressure taps distribution (about 300 orifices on both the upper and lower surfaces), Fig. 1. Elevated Reynolds number values were provided both by the large model size (l/2 = 1724 mm) and by increasing pressure in the setting chamber Po in a range of (1.1 - 2.9)*10⁵ Pa. The model was pressure taped at five spanwise stations (sections 1 - 5). In addition, 11 pressure orifices were placed on the upper surface along the model wing trailing edge (Fig. 1). Pressure orifice diameters were dor. = 0.5 mm. Static pressure at all the tap points was measured simultaneously with a sampling rate of fs = 100 chan/s. In so doing the total sampling time was no more than 3s. Pressure coefficient measurement errors were kept within $\delta_{Cp} \approx 1\%$. During the three-second pressure sampling time mean values of freestream parameters (M, q, P, Po) were obtained by averaging over 17 their current values.

The experimental study on pressure distribution over swept wing section was carried out for a range of Mach numbers from 0.6 to 0.85, a range of mean aerodynamic chord Reynolds numbers Remac from 5 to 20*10⁶ and a range of root chord Reynolds numbers Rel from 9 to 32*10⁶. Angles of attack

measured with respect to the longitudinal fuselage axis of symmetry varied from -1° to $+12^\circ$. Dimensionless maximum cross-section radius was rather large, $2R_f/l = 0.094$.

Analysis of results.

Lifting characteristics. The contributions of various portions of the wing studied to the total lift are not equal. Thus, with a character of chordwise pressure distribution being peak-type, in the subcritical flow regime maximum suction level increases in an outboard direction from $C_{pmin} = -0.92$ at $\bar{z} = 0.114$ to $C_{pmin} = -1.45$ at $\bar{z} = 0.855$. In developed supercritical flow conditions ($M = 0.8$) lift is defined by the presence of an extensive local supersonic region over the entire upper wing surface ($\bar{z} > 0.114$, Fig. 3). Therewith, however, a shock wave does not appear in the root section despite the large thickness-to-chord ratio ($\bar{c} = 15\%$ at $\bar{z} = 0.114$) due to the wing-root effect of a back-swept wing manifesting itself^(4,5). As a consequence of designing the wing with the use of second-generation supercritical airfoils there is a pressure recovered within a local supersonic region at the beginning of the outer wing panel (the section \bar{z} t.e.k. = 0.4 passing through the trailing edge discontinuity point) and the presence of two clearly defined shocks within the middle of near-root wing part ($\bar{z} = 0.24$, Fig. 3).

Section and wing lift coefficients, Cl and CL , were obtained by integrating pressure distributions over wing sections and the entire wing, respectively. It should be noted that in supercritical flow condition the maximum lift in the trailing edge kink section

occurs at an angle of attack of $\alpha = 6^\circ$, whereas for the whole wing it does not take place up to $\alpha = 12^\circ$, Fig. 4. Here by the allowed lift coefficient value (CL_{α}) is meant the one corresponding to the beginning of the nonlinearity of a $CL(\alpha)$ plot.

The variation of wing section lifting capabilities in outboard direction is illustrated in Fig. 5 by the function $Cl_{\alpha}(\bar{z})$.

As one can see, the lifting characteristics of wing sections increase up to the middle of the wing then they decrease both under subcritical ($M = 0.6$) and under supercritical ($M = 0.8 - 0.85$) flow conditions. Therewith in supercritical flow regime the section lifting capabilities over the most part of the wing are higher than those of a flat plate under incompressible flow conditions ($Cl_{\alpha} > 2\pi$). In subcritical flow condition this is not observed ($M = 0.6$, $Cl_{\alpha} < 2\pi$).

It was shown in⁽⁶⁾ numerically that the influence of compressibility (including the cases of developed local supersonic regions) on wing section relative lifting characteristics is practically absent, that is, $Cl_{\alpha}/CL_{\alpha}(\bar{z}) = \text{const}$. Using such a representation of lifting characteristics as applied to the present experiment, one can obtain a single plot Cl_{α}/CL_{α} versus \bar{z} , depicted in Fig. 5.

Local supersonic region and shocks. In cruise flight regimes ($CL = 0.4 - 0.6$, $M > 0.75$) the appearance of local supersonic regions in sections of a supercritical swept wing is favorable to substantially improving its lifting capabilities as compared to those for subcritical flow regimes. For example, when increasing Mach number from 0.6

to 0.85 the lifting capability of the wing increases by 34% (from $CL_{\alpha} = 4.6$ to $CL_{\alpha} = 6.15$, Fig. 5).

Taking the section $\bar{z} = 0.4$ as an example (at $CL = 0.5$), Fig. 6 demonstrates the significant alteration of the character of the flow-field over the upper wing surface as Mach number increases from 0.75 (forward shock position) to 0.85 (shock shifted behind the midchord).

As is generally known, shock waves are the cause of appearing the wing wave drag. The level of the wave drag can be judged by shock strength which is defined by a Mach number value in front of the shock at the surface M_{sh} , Fig. 6. The complex character of the $M_{sh}(M)$ function for the outer part of the wing ($\bar{z} > 0.4$) is governed by the presence of large suction peaks on the forward part of the surface at $M = 0.75$, which weakens with freestream speed (for example, at $\bar{z} = 0.4$). In developed supercritical flow condition at the inner part of the wing ($\bar{z} = 0.24$, $\bar{c} = 14.4\%$) two shocks are observed due to high pre-shock Mach numbers and low trailing edge sweep angle ($\chi_{t.e.} = 7^{\circ}$, see Fig. 3), with the forward one (dashed line in Fig. 6) having $M_{sh} > 1.35$ and the aft one having $M_{sh} < 1.3$.

Based on experimental pressure distributions, the location the shock wave front on the wing surface was determined for two Mach numbers $M = 0.82$ and 0.85 in the cruise flight ($CL = 0.5$ and separated flow ($CL = CL_{al}$) regimes, Fig. 7. It should be pointed out the presence of two shocks on the inner part of the wing ($\bar{z} = 0.24 - 0.386$) and the bending of the shock wave front on the outer part of the wing in separated flow condition ($CL = 0.6, 0.66$).

Boundary layer separation. In the investigation of features of

the flowfield around supercritical airfoil sections of the high-aspect-ratio wing, one of the principal items is the question about the presence of boundary layer separation, in particular at cruise conditions. As evidenced by studies of two-dimensional flows using various sophisticated methods (7) for determining separation onset based on the change in the behavior of the static pressure coefficient at the trailing edge $C_{pt.e.}$ as a function of angle of attack. This separation onset criterion was used in the investigation of three-dimensional flow around sections of the swept high-aspect-ratio wing (Fig. 8). The arrows in Fig. 8 designate the values $\alpha = \alpha_{sep}$ for which $C_{pt.e.} > 0$.

Based on the α_{sep} values and the lifting properties of the wing and its sections, the wing lift coefficient CL_{sep} corresponding to the separation onset conditions is plotted in Fig. 9 against dimensionless spanwise location \bar{z} for $M = 0.8$. Plotted here are also the maximum allowed section lift coefficients Cl_{al} (that is, corresponding to onset of nonlinearity in the $Cl(\alpha)$ relationship) as function of \bar{z} for $M = 0.60 - 0.85$.

It should be noted that the thickened supercritical swept wing at the cruise value $CL = 0.5$ and $M = 0.75 - 0.85$ has attached flow at $Re > 7 \cdot 10^6$. At $CL \approx CL_{al}$ for a wide Mach number range of $M = 0.75 - 0.85$ separated flow occurs mainly on the outer part of the wing ($\bar{z} > 0.4$). On the inner part of the wing ($\bar{z} < 0.4$, $\bar{c} = 13 - 15\%$) at these conditions flow is attached up to $CL \approx 0.75 - 0.55$.

Analysis of the lifting properties of wing sections shows that the location of the maximum $Cl_{al}(\bar{z})$ at $M = \text{const}$ corresponds to a section

beginning from which ($\bar{z} > \bar{z}_{sep}$) there is separated flow appropriate to the $CL = CL_{al}$. regime (Fig. 9).

To summarize the results of the wing separated flow investigations, the $CL_{sep}(M)$ and $\bar{z}_{sep}(M)$ relationships are presented in Fig. 10. It can be seen that the boundary layer separation does not occur on the thick supercritical wing considered up to $CL = 0.70 - 0.41$. At $CL = 0.55$ and $M = 0.75 - 0.80$ the separation takes place only on the tip part of the wing ($\bar{z}_{sep} > 0.8$). At $CL \approx CL_{al}$ and $M = 0.6 - 0.83$ the boundary layer separation is observed only on the outer part of the wing.

At $M > 0.83$ the separation partially occupies the inner part of the wing as well (up to $\bar{z} \approx 0.35$ at $M = 0.85$).

Scale effects. Consider the effect of Reynolds number on the distributed characteristics of the sections of the thick supercritical swept high-aspect-ratio wing in regimes of attached and separated flows at local chord Reynolds numbers of $Re \approx (7 - 32) * 10^6$.

For attached supercritical flow around this wing (for example, $\bar{z} = 0.4$, $M = 0.82$) the increase in the Reynolds number in the range of $Re = (10.2 - 17.2) * 10^6$ results mainly in a shock-wave shift, $x_{sh} = 0.50 - 0.56$, Fig. 11.

The maximum scale effects take place, as in the case of two-dimensional flow ⁽¹⁾ presence of boundary layer separation in various wing sections. It is clearly observed at a Mach number close to the cruise value ($M = 0.82$) in the regime of a fully pronounced separated flow ($CL = 0.65 \approx CL_{al}$) in the section $\bar{z} = 0.4$ ($\bar{c} = 13\%$) at the beginning of outer part of the wing, Fig. 12. It can be seen that the increase in the

Reynolds number in the range of $Re = (7.6 - 20.5) * 10^6$ noticeably suppresses separation in the rear part ($\bar{x} > 0.7$) of wing section (Cpt.e. = -0.13 to $+0.11$) thus promoting a downstream shock-wave shift ($\Delta \bar{x}_{sh} \approx 0.05$).

For a substantially supercritical flow about the inner part of the wing ($M = 0.85$, $\bar{z} = 0.114 - 0.24$) at CL_{al} the flow remains attached at $Re = (17 - 32) * 10^6$, Fig. 13. In a section near the trailing-edge kink ($\bar{z} = 0.4$) the influence of the Reynolds number in the range of $Re = (9.8 - 21) * 10^6$ on the attenuation of separation and downstream shock-wave shift is rather noticeable, Fig. 13. On the outer part of the wing because of an intensive separation the increase in Reynolds numbers from $Re = 9.5 * 10^6$ to $15 * 10^6$ does not lead to an improved flow, as it can be seen in the two-dimensional case

Fig. 14 presents the generalized relationships Cpt.e.(Re) and $\bar{x}_{sh}(Re)$ for the section with $\bar{c} = 13\%$ at $\bar{z} = 0.4$ for attached ($CL = 0.55$) and separated ($CL \approx CL_{al} = 0.65$) flows.

In the case of attached flow, the increase in Reynolds number from $10.2 * 10^6$ to $17.2 * 10^6$ results in a small pressure recovery near the trailing edge (Cpt.e. = $0.13 - 0.15$). For the separated flow case the Reynolds number increase from $Re = 7.6 * 10^6$ to $20.5 * 10^6$ practically totally suppresses flow separation (Cpt.e. = -0.13 to $+0.11$).

For the attached flow the shock wave shifts downstream and its chordwise position stabilizes already at $Re = 13.7 * 10^6$. If the flow is separated ($CL \approx 0.65$, the increase from $Re = 7.6 * 10^6$ to $20.5 * 10^6$ leads to a gradual

shift of the shock downstream ($\bar{x}_{sh} = 0.48 - 0.53$).

Conclusions.

1. The experimental investigation of the transonic aerodynamics ($M = 0.6 - 0.85$) of the thick supercritical swept high-aspect-ratio wing at angles of attack from -1° to 12° and Reynolds numbers up to $Re_{max} = 32 \cdot 10^6$ was conducted using a large-scale, pressure tapped semi-span wing-body model (semispan 1754 mm).

2. In a subcritical Mach number range of $M = 0.75 - 0.85$ the supercritical wing tested has high lifting properties. The maximum lift coefficient is not reached up to $\alpha = 12^\circ$. It is shown that there is no compressibility effects on the lift section lifting properties in the presence of local developed supersonic zones.

3. For developed supercritical flows ($M > 0.8$, $CL > 0.4$) on the inner part of the wing ($z < 0.4$) there are two shocks caused by a high local Mach number on the surface ahead of the shocks ($M_{sh} > 1.35$) together with a low trailing-edge sweep ($\chi_{te} = 7^\circ$).

4. The investigation of attached and separated flows showed that at the cruise value $CL = 0.5$ the thick supercritical swept wing under study has an attached-flow regime in the Mach number range of $M = 0.75 - 0.82$.

5. The regime of nonlinearity onset for the relationship $CL(\alpha)$ (when $CL = CL_{al}$) features boundary-layer separation only on the outer part of the wing ($\bar{z} > 0.4$) in a wide Mach number range of $M = 0.75 - 0.85$. It is found that the maximum of $Cl_{al}(\bar{z})$ at $M = \text{const}$ is reached at the section after which up to wing tip ($\bar{z} > \bar{z}_{sep}$) there is separated flow corresponding to the regime $Cl = Cl_{al}$.

6. The increase in Reynolds number up to $Re_{max} \approx 32 \cdot 10^6$ in

supercritical flow regimes ($M > M_{cr}$) results in a downstream shock-wave shift ($\Delta \bar{x}_{sh} \approx 0.05$) and the practically total suppression of boundary layer separation in certain wing sections. For example, at $\bar{z} = 0.4$, $CL = 0.65$, $M = 0.82$ the increase in Reynolds number from $7.6 \cdot 10^6$ to $20.5 \cdot 10^6$ practically totally recovers the static pressure at the trailing edge, $C_{pt.e.} = -0.13$ to $+0.11$.

References

1. V.D. Bokser, V.M. Gadetsky, V.G. Knivel, I.V. Makarevich. Transonic flow about an airfoil at high Reynolds numbers, Uchenye Zapiski TsAGI, v.11, No 1, 1980 (in Russian).
2. V.M. Gadetsky. Experimental investigation of the effect of Reynolds number on the flow around a swept wing at transonic speeds, Uchenye Zapiski TsAGI, v.19, N 1, 1988 (in Russian).
3. S. Agrawal, R.B. Lowrie, S.F. Creasman. An evaluation of Euler solvers for transonic flowfield computations on wing-fuselage geometries, AIAA Paper, N-90-3015, 1990.
4. V.D. Bokser, L.N. Kirillov, K.S. Nikolaeva, Ya.M. Serebriisky. Transonic flow around the root section of a swept wing. Uchenye Zapiski TsAGI, v.12, No.1, 1981 (in Russian).
5. Ya.M. Serebriisky, V.D. Bokser, K.S. Nikolaeva, L.N. Kirillov. Experimental investigation of flowfield features around the root section of a swept wing in the presence of lift, Trudy TsAGI, issue 2161, 1982 (in Russian).
6. V.D. Bokser, N.A. Vladimirova. Features of lift capability of a swept wing in a compressible gas ($M < 1$), Uchenye Zapiski TsAGI, v.24, No.3, 1993 (in Russian).
7. V.D. Bokser. Development of separation and its influence on aerodynamics of supercritical

airfoils at transonic speeds.
 Uchenye Zapiski TsAGI, v.19.
 No.5, 1988 (in Russian).

| sect. | 1 | 2 | 3 | 4 | 5 |
|-------------------------|-------|-------|-------|-------|-------|
| $\bar{z} = \frac{z}{c}$ | 0.114 | 0.240 | 0.400 | 0.627 | 0.855 |
| b [mm] | 641 | 530 | 393 | 300 | 206 |

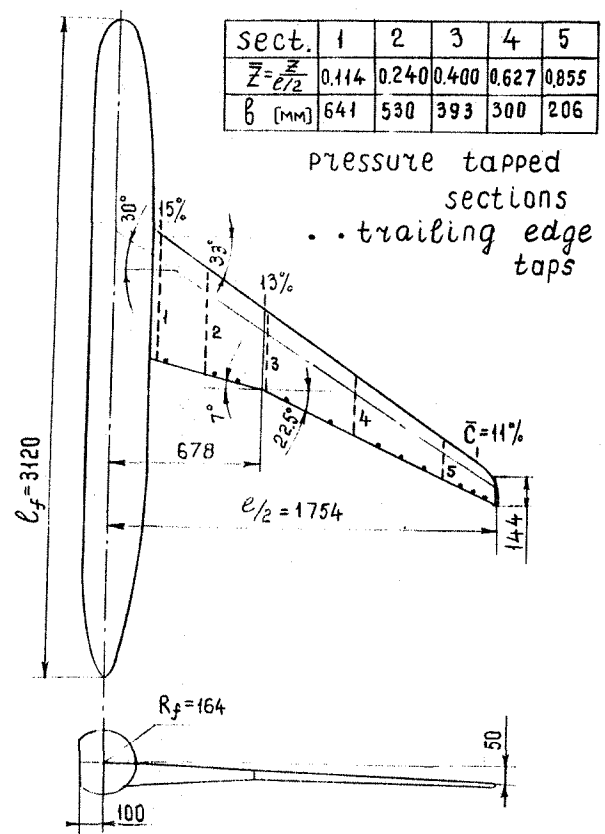
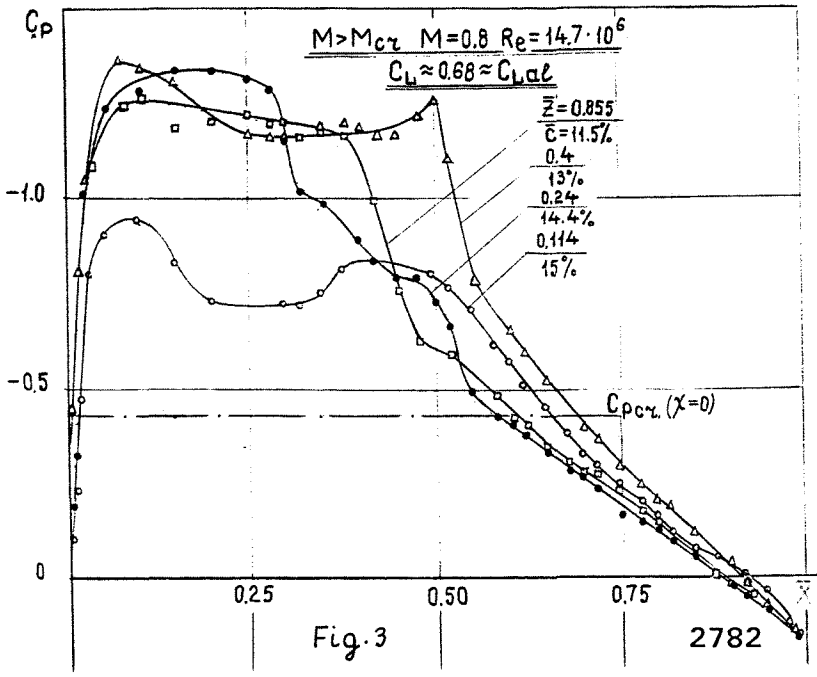
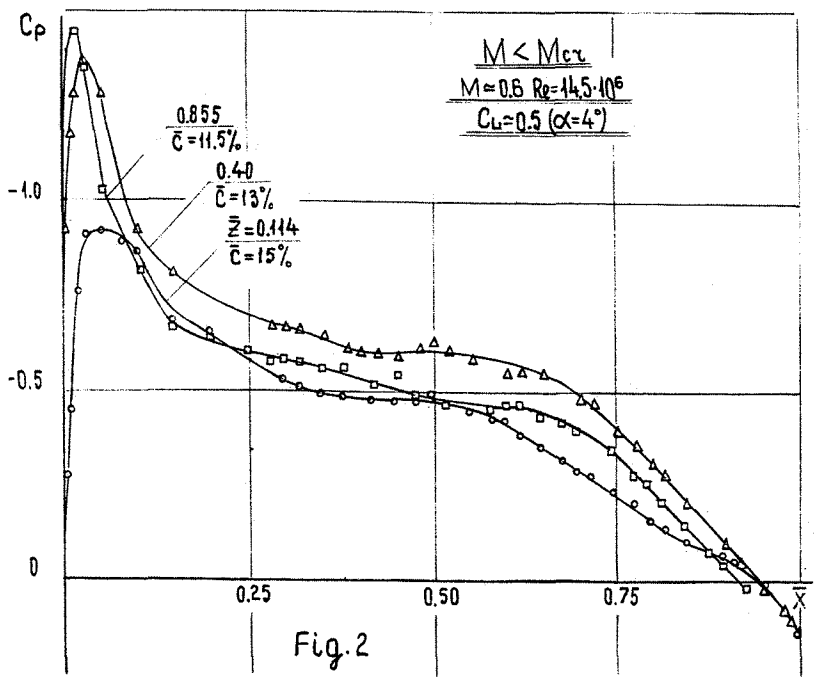


Fig. 1



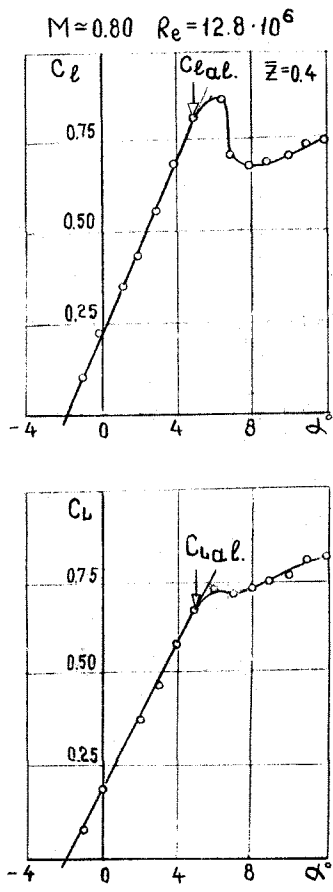


Fig. 4

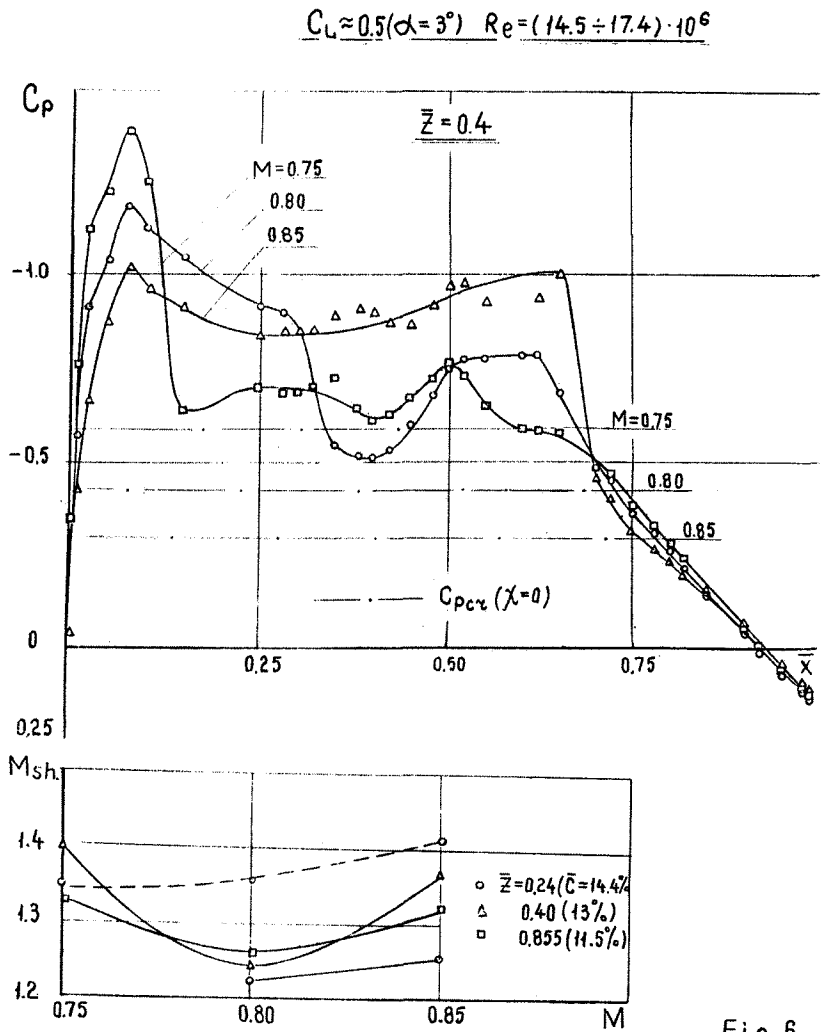


Fig. 6

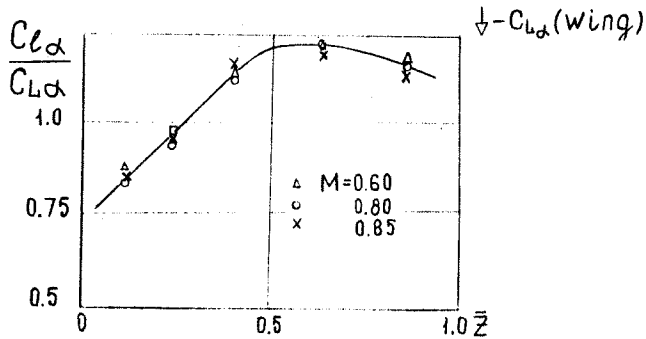
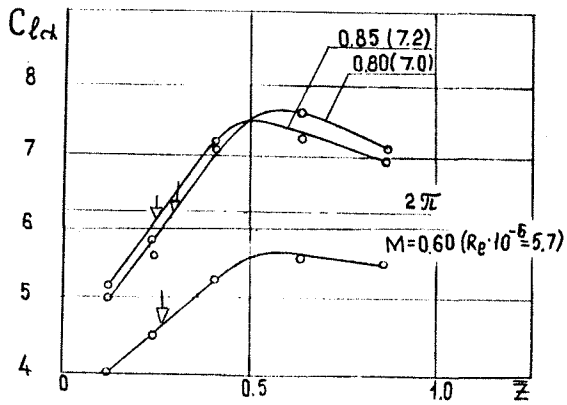
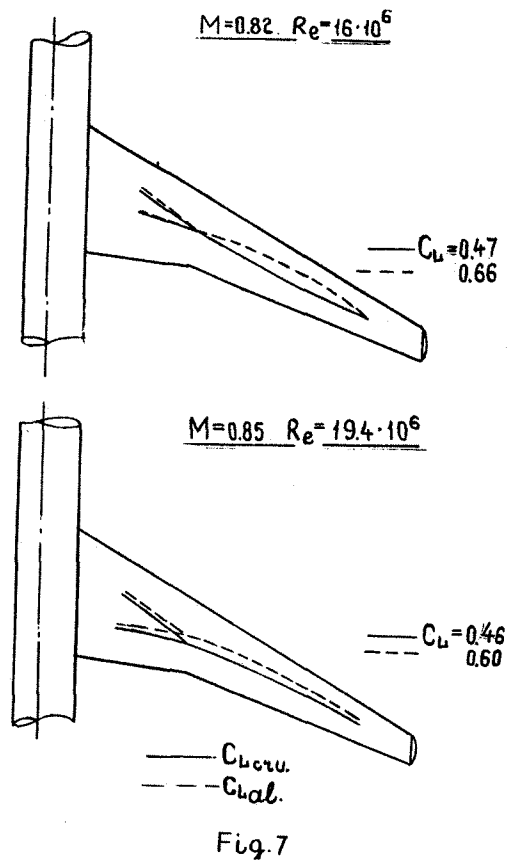


Fig. 5



$M=0.80 \quad Re=12.8 \cdot 10^6$

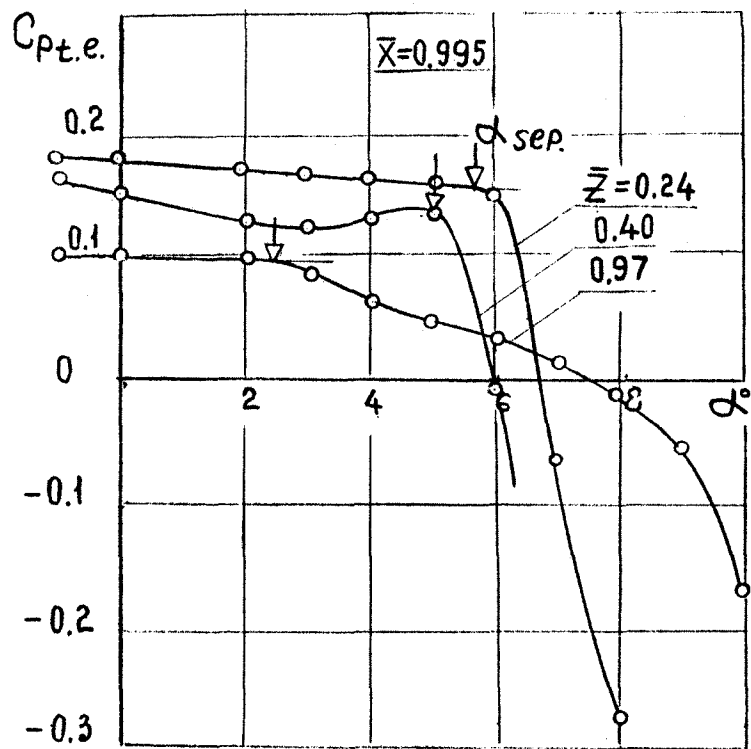
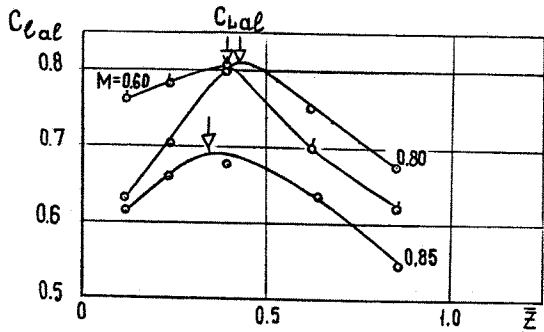
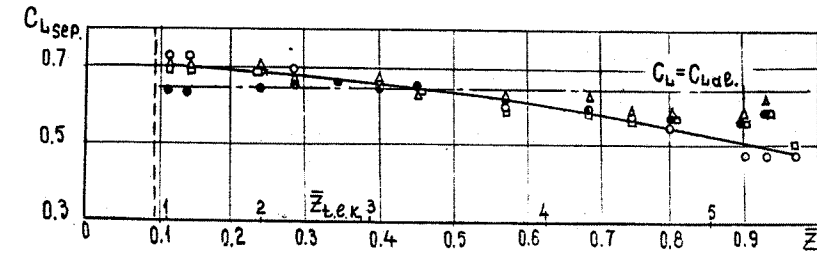


Fig. 8

$$M=0.80 (Re=7 \cdot 10^6 \div 16 \cdot 10^6)$$



$Re \cdot 10^{-6}$
 Δ 7.0 --- root section
 \circ 9.1 1/5 - pressure tapped sections
 \square 13.0
 \bullet 16.0

Fig. 9

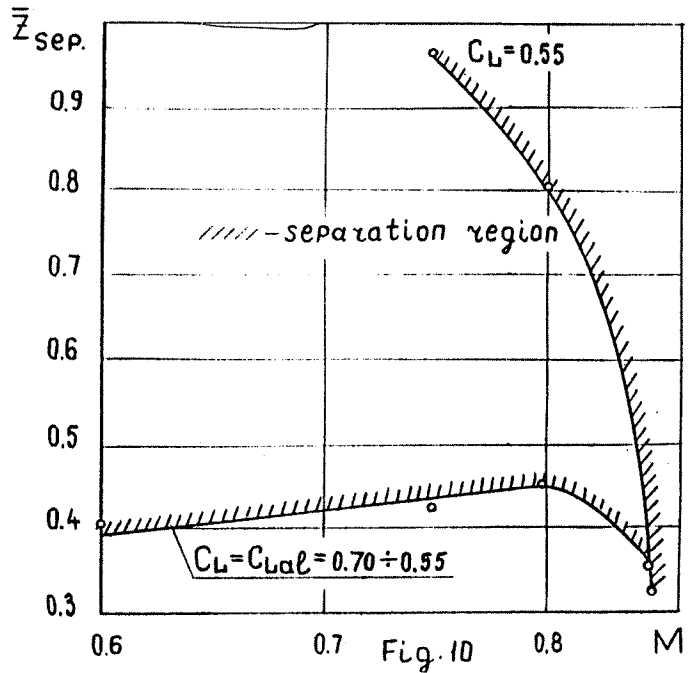
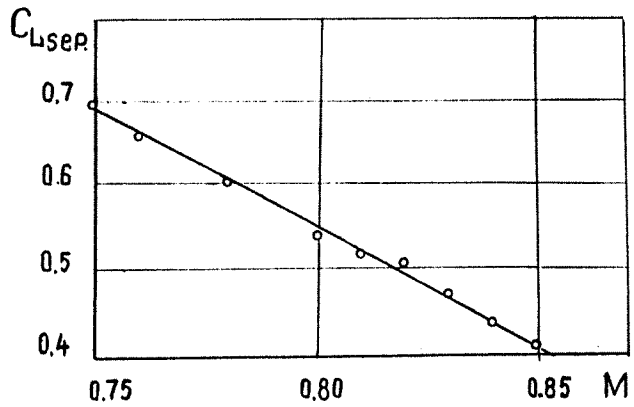


Fig. 10

